



OPEN Novel histone deacetylase-5 inhibitor T2943 exerts an anti-depressive effect in mice by enhancing GRID1 expression

Juan Du^{1,2}, Ruyun Liu¹, Lin Ma¹, Yue Liu¹, Wei Wei¹, Ning Liu^{1,2}✉, Qiuhua Cao³✉ & Jianqiang Yu¹✉

Histone deacetylase-5 (HDAC5) is implicated in the pathogenesis of depression and the mechanistic pathways underlying the effects of antidepressant medications. We previously identified a novel HDAC5 inhibitor, T2943, with antidepressant properties that promote histone 3 lysine-14 acetylation (H3K14ac) by inhibiting HDAC5 activity. In this study, we identify the core genes promoting transcription and expression following T2943-mediated upregulation of H3K14ac, highlighting *Grid1* (*GluD1*) as a central gene. We used cleavage under targets and tagmentation (CUT&Tag), gene set enrichment analysis, and behavioral tests after GRID1 (glutamate receptor delta-1 subunit) knockdown. Gene ontology and pathway enrichment analysis via CUT&Tag suggested the following mechanism for the antidepressant action of T2943: T2943 inhibits HDAC5 activity to promote H3K14 acetylation. This modification loosens the chromatin structure, allowing transcription factors to bind to the *Grid1* promoter region and enhance its transcription and expression. Upregulated GRID1 mediates signal transmission in neural pathways, restores the regenerative ability of hippocampal nerve cells, promotes nerve growth and synaptic formation, increases synapse numbers, and enhances synaptic function. Our findings highlight the therapeutic potential of targeting HDAC5 in depression and clarify the antidepressant mechanism of T2943.

Keywords Histone deacetylase-5 inhibitor, T2943, Depression, Histone acetylation, Epigenetics

Depression is a severe mood disorder often characterized by recurrent episodes of sadness and accompanied by anhedonia, decreased concentration and energy, loss of appetite, guilt, and suicidal thoughts, which seriously affect the quality of life of patients¹. Treatments for depression, especially major depressive disorder, remain inadequate and have limited therapeutic effects². Most antidepressants currently used in clinical practice require long-term intake, and despite that, more than 50% of patients experience relapse, with a high recurrence rate³. Therefore, an in-depth understanding of the pathogenesis of depression and the development of new antidepressants is urgently needed.

Depression is influenced by environmental factors⁴, such as early adverse experiences, stressful events, and emergencies^{5–7}. Both genetic susceptibility and environmental factors work concomitantly to cause depression⁸. Epigenetics bridges genes and environmental factors⁹ and refers to the “heritable but reversible regulation of various genome functions mediated mainly through DNA methylation and changes in chromatin structure”¹⁰. Epigenetic regulatory mechanisms include histone modification, DNA methylation, non-coding RNA regulation, and chromatin remodeling¹¹, which have become research hotspots in the field of psychiatry. Histone acetylation plays an important role in depression pathophysiology and regulates interactions between histones and DNA at the local level via histone acetyltransferases (HATs) and histone deacetylases (HDACs).

In addition, acetylation and deacetylation of non-histone proteins by HATs and HDACs regulate various cellular functions¹². Altered HDAC expression is associated with diseases, such as cancer¹³, depression^{14,15}, Alzheimer’s disease¹⁶, diabetes^{17,18}, and chronic obstructive pulmonary disease¹⁹. The HDAC family is divided into four classes: class I, which includes HDAC1, HDAC2, HDAC3, and HDAC8; class IIa, which includes

¹Department of Pharmacology, School of Pharmacy, Ningxia Medical University, Yinchuan, China. ²Key Laboratory of Protection, Development and Utilization of Medicinal Resources in Liupanshan Area, Ministry of Education, School of Pharmacy, Ningxia Medical University, Yinchuan, China. ³Vaccine Center, School of Basic Medicine and Clinical Pharmacy, China Pharmaceutical University, Nanjing, China. ✉email: 20160126@nxmu.edu.cn; 1520210058@cpu.edu.cn; 19870041@nxmu.edu.cn

HDAC4, HDAC5, HDAC7, and HDAC9; class IIb, which includes HDAC6 and HDAC10; class III, which includes silent information regulator 2 and its related enzymes; and class IV, the main member of which is HDAC11²⁰. Studies have confirmed that HDAC5 levels are highly correlated with depression^{14,21,22} and that HDAC5 expression in the dentate gyrus (DG) region of the mouse hippocampus promotes depression^{23,24}. Therefore, the development of novel HDAC inhibitors for the treatment of depression is of great interest.

Earlier, we employed virtual screening technology and HDAC5 inhibitor screening to assess the HDAC5 inhibitory activity of 199 compounds, and we identified T2943 as a novel HDAC5 inhibitor with an antidepressive effect, through behavioral experiments, such as forced swimming test, tail suspension test, open field test, and sucrose preference test²⁵. Histone acetylation proteomic analysis indicated that T2943 upregulates H3K14 acetylation by inhibiting HDAC5²⁵, indicating that T2943 exerts its antidepressive effect by regulating gene expression; however, it remains unclear which genes are transactivated in response to H3K14 acetylation. Therefore, in this study, we aimed to use cleavage under targets and tagmentation (CUT&Tag) technology and gene set enrichment analysis (GSEA) to screen the core genes and proteins associated with T2943-regulated H3K14ac expression and verify and analyze these molecules using molecular techniques including PCR and immunofluorescence. Finally, we sought to elucidate the mechanism underlying the anti-depressive effects of T2943.

Methods

Animals

Adult male Bl6/C57 mice (8–10 weeks old; Laboratory Animal Center, Ningxia Medical University, Yinchuan, China) were individually housed and maintained under a 12-h light–dark cycle with ad libitum access to food and water. This experimental study was approved by the Ethics Committee of Ningxia Medical University Animal Experiments Local Ethics Committee (2021-N0065). And the entire study was conducted in accordance with the Animal Experiments Local Ethics Committee Directive. All animal experiments were performed in accordance with ARRIVE guidelines.

Injections

Mice were anesthetized with an intraperitoneal injection of 0.3% pentobarbital (50 mg/kg) and fixed on a brain stereotaxic instrument (RWD Life Science Co., Ltd., Shenzhen, China). The Injection method was following the same strategy as before²⁵. After disinfecting the mouse head with iodophor, the fur on the head was removed using a pair of curved scissors, and the scalp was cut along the sagittal position using a pair of straight scissors to expose the skull. The bregma position of the mouse fontanelle was carefully confirmed and considered point 0. According to the stereotaxic map of the mouse brain, the coordinates of the DG region of the mouse hippocampus were determined (anterior–posterior [AP]: – 2.18 mm; medial–lateral [ML]: ± 1.4 mm). A micro-dose cannula (RWD Life Science Co., Ltd.) was placed at a suitable depth on the dorsoventral (DV) side of – 1.8 mm using a clamp²⁵.

T2943 solution (10 µg/µL; Shanghai Topscience Co., Ltd., Shanghai, China) was injected with a micro-syringe into the bilateral drug delivery cannula at an injection rate of 500 nL/min. The needle remained in place for 5 min after the injection. The “T2943” treatment group received 4 µL T2943 (10 µg/µL) once a day for 10 days²⁵.

Chronic restraint stress model mice

C57BL/6J male mice were acclimated at a suitable temperature 23 ± 2 °C for 1 week, the mice were randomly categorized into the normal and chronic restraint stress (CRS) model groups. The mice in the CRS group were confined to a 50-mL centrifuge tube for 4 h a day (10:00–14:00) for 28 days²⁵.

Mouse hippocampal tissue specimens

The mice were anesthetized by forced inhalation of isoflurane. The heads were quickly cut with tissue scissors, and the brain tissue was stripped and thoroughly rinsed. Next, the hippocampal tissue was separated using a glass dissecting tool, rinsed with normal saline, placed in a sterile 1.5-mL centrifuge tube, and stored in liquid nitrogen. Hippocampal tissue samples were obtained from mice in the model group and the T2943 treatment group. Two samples were obtained from each group²⁵.

Cleavage under targets and tagmentation (CUT&Tag) analysis

Cells (10 × 10⁵) were washed twice gently with wash buffer (20 mM HEPES (pH 7.5); 150 mM NaCl; 0.5 mM Spermidine; 1 × Protease inhibitor cocktail) and incubated with concanavalin A-coated magnetic beads (10 µL; Bangs Laboratories) at 23 °C ± 2 °C for 10 min. Unbound fraction was removed and bead-bound cells were incubated overnight with the primary antibody (anti-H3K14ac) or IgG control antibody (normal mouse IgG; cat.no. 12-371; Millipore) diluted 1:50 with dig wash buffer (20 mM HEPES (pH 7.5); 150 mM NaCl; 0.5 mM Spermidine; 1 × Protease inhibitor cocktail; 0.05% Digitonin; 2 mM EDTA) on a rotating platform at 4 °C. The primary antibody-bound cells were collected by placing the mixture on a magnet stand. These cell were then incubated with the secondary antibody (Rabbit Anti-Mouse IgG H&L diluted 1:100 in dig wash buffer; ab611709; Abcam) at RT for 60 min. Then, cells were washed 2–3 times with dig wash buffer by placing the mixture on a magnetic stand. The cells were then incubated with a 1:100 dilution of pA-Tn5 adapter complex in dig-med buffer (0.01% Digitonin; 20 mM HEPES (pH 7.5); 300 mM NaCl; 0.5 mM Spermidine; 1 × Protease inhibitor cocktail) at RT for 1 h. They were then washed 2–3 times for 5 min with 1 mL Dig-med buffer. Afterward, the cells were incubated with tagmentation buffer (10 mM MgCl₂ in Dig-med Buffer) at 37 °C for 1 h. DNA was purified using phenol–chloroform–isoamyl alcohol extraction and ethanol precipitation. To amplify the libraries, 21 µL DNA was mixed with 2 µL of a universal i5 and a uniquely barcoded i7 primer. Then, 25 µL NEBNext HiFi 2 × PCR Master mix was mixed with this mixture. PCR was performed on a Thermocycler with a heated lid under the

following cycling conditions: 72 °C for 5 min (gap filling); 98 °C for 30 s; 14 cycles of 98 °C for 10 s, and 63 °C for 30 s; final extension at 72 °C for 1 min, and hold at 8 °C. Library clean-up was performed using XP beads (Beckman Counter). Peak calling was performed using MACS2 software with a cut-off q -value of <0.05 . The peaks were annotated with annotated peak functions using the ChIPseeker R package. Differential peaks were assessed with the DESeq2 R package ($|\text{fold change}| \geq 2$, $P < 0.05$). H3K14ac signals in the chromosomes were visualized using the Rideograms R package. The raw sequence data reported in this paper have been deposited in the Genome Sequence Archive (Genomics, Proteomics & Bioinformatics 2021) in National Genomics Data Center (Nucleic Acids Res 2022), China National Center for Bioinformation / Beijing Institute of Genomics, Chinese Academy of Sciences (GSA: CRA018661); they are publicly accessible at <https://ngdc.cnbc.ac.cn/gsa/search?searchTerm=CRA018661>

Gene set enrichment analysis

GSEA is a computational method that determines whether a priori-defined set of genes shows statistically considerable and concordant differences between two biological states (e.g., phenotypes). Enrichment analyses were conducted to determine whether a series of priori-defined biological processes were enriched. The enriched pathways were arranged in the order of their normalized enrichment scores (ESs), and 6665 genes were found in the database. Genes with $P < 0.01$ and $\text{FDR} < 0.25$ were selected for further analysis. The GSEA results for different expression profile datasets were intersected to obtain the common significant Kyoto Encyclopedia of Genes and Genomes (KEGG) pathways, and the core gene sets were analyzed.

Gene ontology analysis

Gene ontology (GO) analysis was performed to elucidate the biological implications of the unique genes in the significant gene profiles. We annotated the genes associated with accessible chromatin regions using the Genomic Regions Enrichment of Annotations Tool (GREAT, v.3.0.0)²⁶. The annotated genes were then analyzed based on GO annotations in the database. The significance level of each ontology was calculated using Fisher's exact test. Statistical significance was set at $P < 0.05$.

Pathway analysis

Pathway analysis was performed to explore annotated genes and differentially enriched gene signaling pathways. The annotated and differentially expressed genes were analyzed using the Kyoto Encyclopedia of Genes and Genomes database to obtain all involved pathway terms. The significance level of each pathway term was calculated using Fisher's exact test. Statistical significance was set at $P < 0.05$.

qRT-PCR

The RNAsimple Total RNA Kit (Cat. #DP419 Lot#W9528; TIANGEN, Beijing, China) was used to obtain RNA from tissues after cutting, extraction, rinsing, and elution following the standard protocol as described before²⁵. The RNA concentration was determined using a NanoDrop 2000 spectrophotometer (Thermo Fisher Scientific, Waltham, MA, USA). A PrimeScript™ RT Reagent Kit with a gDNA Eraser (Perfect Real Time) (Code No. RR047A; Takara Bio, Tokyo, Japan) was used for removing genomic DNA and performing reverse transcription²⁵. The cDNA template was obtained for qPCR. PCR was performed with a TB Green® Premix Ex. Taq™ II (TliRNase H Plus) kit (Code No. RR820A; Takara Bio) with the following primers: *Grid1* forward (5′–3′), GCA GGA AGA ACC ATC GGA GAA G; reverse (5′–3′), CCA AGG ACA 6G ACTT GAG GAA TGA G; *Grid2* forward (5′–3′), CCT GGT CAA GCG TAC TCA CAC TG; reverse (5′–3′): GGC ACA 6G ACTT TTG GTC CTT CAC; *Gapdh* forward (5′–3′), GGT TGT CTC CTG 6G ACTT CA; reverse (5′–3′), TGG TCC AGG GTT TCT TAC TCC. PCR was performed on a Thermocycler with a heated lid under the following cycling conditions: 95 °C for 30 s, 95 °C for 5 s, 58 °C for 30 s, 95 °C for 10 s, 65 °C for 5 s, 95 °C for 5 s.

Western blotting

Mouse hippocampal lysates were prepared using a total protein extraction kit containing protease and phosphatase inhibitors (KeyGEN Biotech Corp., Ltd., Nanjing, China)²⁵. Protein concentrations were determined using a Pierce BCA Protein Assay Kit (Thermo Fisher Scientific) following the same strategy as before²⁵. Proteins (20 µg) were separated using an SDS-PAGE Gel Rapid Preparation Kit to prepare 12% SDS–polyacrylamide gels (Wuhan Servicebio Co., Ltd., Wuhan, China) and transferred onto polyvinylidene fluoride membranes. The membranes were subsequently blocked with 0.1% Tween 20/phosphate saline (PBST) containing 5% bovine serum albumin, followed by incubation with anti-GRID1 (1:1,000; Thermo Fisher Scientific) or anti-β-actin (1:20,000; Affinity Biosciences, Cincinnati, OH, USA) antibodies overnight at 4 °C. Membranes were washed with PBST 3 times (10 min each wash) while avoiding light exposure. Then, the membranes were incubated with horseradish peroxidase-conjugated anti-rabbit IgG (1:10,000; Abcam, Cambridge, UK) and washed using the method described above. The blots were developed using an Odyssey two-color infrared fluorescence imaging system (LI-COR Biosciences, Lincoln, NE, USA). The density of the immunoreactive bands was measured using ImageJ 1.53q software (NIH, Bethesda, MD, USA). GRID1 to β-actin ratio was used to quantify GRID1 expression in each group, thereby confirming its association with H3K13 acetylation modification.

Immunofluorescence

For immunofluorescence, mice were deeply anesthetized with sodium pentobarbital and perfused transcardially with phosphate-buffered saline (PBS, 0.1 M, pH 7.4), followed by phosphate-buffered 4% paraformaldehyde (PFA)²⁵. Their brains were rapidly removed, post-fixed overnight in phosphate-buffered 4% PFA, and equilibrated in 30% sucrose for 2 days. The brain tissues were fixed on a thermostatic freezing microtome, cut into slices of 4 µm thickness, and mounted on slides; the slides were placed in a dark box to dry²⁵. The sections were placed in

antigen retrieval solution, microwave-fired for 7 min, and incubated at room temperature for 30 min to 1 h. The slices were washed in PBST three times for 5 min each, placed in a PBS solution mixed with 0.1% Triton X-100 for 3 h, and then blocked with 1% bovine serum albumin for 1 h. Circles were drawn around the brain tissue sections with a histochemical pen, and then the primary antibody (approximately 200 μ L anti-GRID1) was dropped into the circles and incubated at 4 °C overnight²⁵. The brain sections were washed three times in PBST for 5 min each time. Afterward, the secondary antibody was added and incubated at RT for 3 h, and the brain sections were washed three times in PBST for 5 min each time. Finally, an anti-fluorescence attenuator (such as 4',6-diamidino-2-phenylindole) was added²⁵ and the slides were sealed with CoverGrip Coverslip Sealant (Biotium, CA, USA).

Tail suspension test

For the tail suspension test (TST), the mice were suspended by bands on the edge of a 20-cm high floor. The time spent immobile during the 5-min testing period was measured using a video recorder (RWD Life Science Co., Ltd., Shenzhen, China) and Smart 3.0 small animal behavior tracking and analysis system (Panlab, Barcelona, Spain). Immobility time was defined as the lack of any movement, except whisker movements and respiration²⁵.

Open field test

To assess locomotor activity, an open field test (OFT) was performed. Briefly, the mice were placed at the center of a box (50 cm \times 50 cm \times 35 cm) and allowed to explore for 5 min. The performance of each mouse was recorded using a video tracking system (RWD Life Science Co., Ltd.). The test room was dimly lit using indirect white light²⁵.

Sucrose preference test

The sucrose preference test (SPT) was performed in a quiet environment. Before the formal experiment, the mice received two bottles of 1% sucrose solution (Sinopharm, Shanghai, China) for 24 h²⁵. One bottle was replaced with pure water and the mice were allowed to adapt for 24 h. The positions of the two bottles were exchanged after 12 h. The mice were deprived of food and water for 24 h before the test and provided a pre-weighed bottle of 1% sucrose solution and a bottle of pure water for a 36-h formal test²⁵. The weights of the two bottles with the remaining solution were recorded after 0, 12, 24, and 36 h to calculate the sucrose preference percent:

$$\text{Sucrose preference (\%)} = \frac{\text{Sucrose consumption}}{\text{Sucrose consumption} + \text{Water consumption}} \times 100\%$$

Knockdown of Grid1 expression

One group of mice was treated with hippocampal injection of AAV-shGRID1 (1.0 \times 10¹² vg/mL, 0.5 μ L) maintained for 2 weeks in order to knock down GRID1 (shGRID1 mouse model). Another group of mice was treated with hippocampal injection of AAV-shControl (1.0 \times 10¹² vg/mL, 0.5 μ L) and maintained for 3 weeks (shControl mouse model). The mice were euthanized after 2 weeks of treatment, and hippocampal tissue specimens were collected for the evaluation of the behavioral experiment.

Statistical analysis

Data were analyzed using GraphPad Prism version 9 (GraphPad Software, San Diego, CA, USA) and are expressed as mean \pm standard deviation. A two-way analysis of variance was used. Statistical significance was as follows: * P < 0.05, ** P < 0.01, *** P < 0.001, and **** P < 0.0001.

Results

CUT&Tag analysis of the hippocampi of the depression model and T2943 groups

We screened the gene fragments that bound to the acetylated H3K14. The similar distribution of the fragment sizes suggested that chromatin was accessible to Tn5 transposase to the same degree in all samples independently between different groups (Fig. 1a). Integration analysis of H3K14ac binding sites in the hippocampi of mice showed that 18,807 and 18,617 binding sites were occupied in the depression model and T2943 groups, respectively, corresponding to 11,165 and 11,838 genes, respectively (Fig. 1b).

We normalized all genes according to length, used deepTools (tools for exploring deep sequencing data) software to calculate the average signal value of genes at each locus from 3 kb upstream and 3 kb downstream of the transcriptional end site (TSS), and obtained the read signal distribution across all genes. The average signal of each group showed a strong signal peak near the TSS, suggesting that the gene fragments obtained were mainly concentrated in that area (Fig. 1c).

To investigate the functional role of the chromatin accessibility region in regulating gene expression, signaling pathways, and gene function after T2943 inhibited HDAC5 and upregulated H3K14ac expression, we analyzed different pathways and biological processes in mice in the depression model and T2943 groups. GO enrichment analysis was used to identify GO entries significantly enriched near peak genes, thereby demonstrating gene functions that may be regulated by transcription factors. All peak-adjacent genes were assigned to different GO functional categories at three levels, namely molecular function (MF), biological process (BP), and cellular component (CC). The top 20 results of T2943 upregulated differential peak-adjacent gene enrichment in MF, BP, and CC are presented in Fig. 2a–c. In the T2943 group, the upregulated genes related to BP were mainly involved in the regulation of signaling and cell communication, which are mainly associated with protein binding, gated channel activity, cell junctions, and synapses in the MF and CC. We also measured the GO enrichment degree of T2943 upregulated genes using the Rich factor, P value, and the number of genes enriched in the GO entry through the bubble map of peak-adjacent genes. Among the upregulated differentially expressed genes in the T2943 vs. model group, the significance of the P value of the enriched genes in the GO entry for signaling regulation was the smallest, indicating that this GO entry was the most significantly enriched. Therefore,

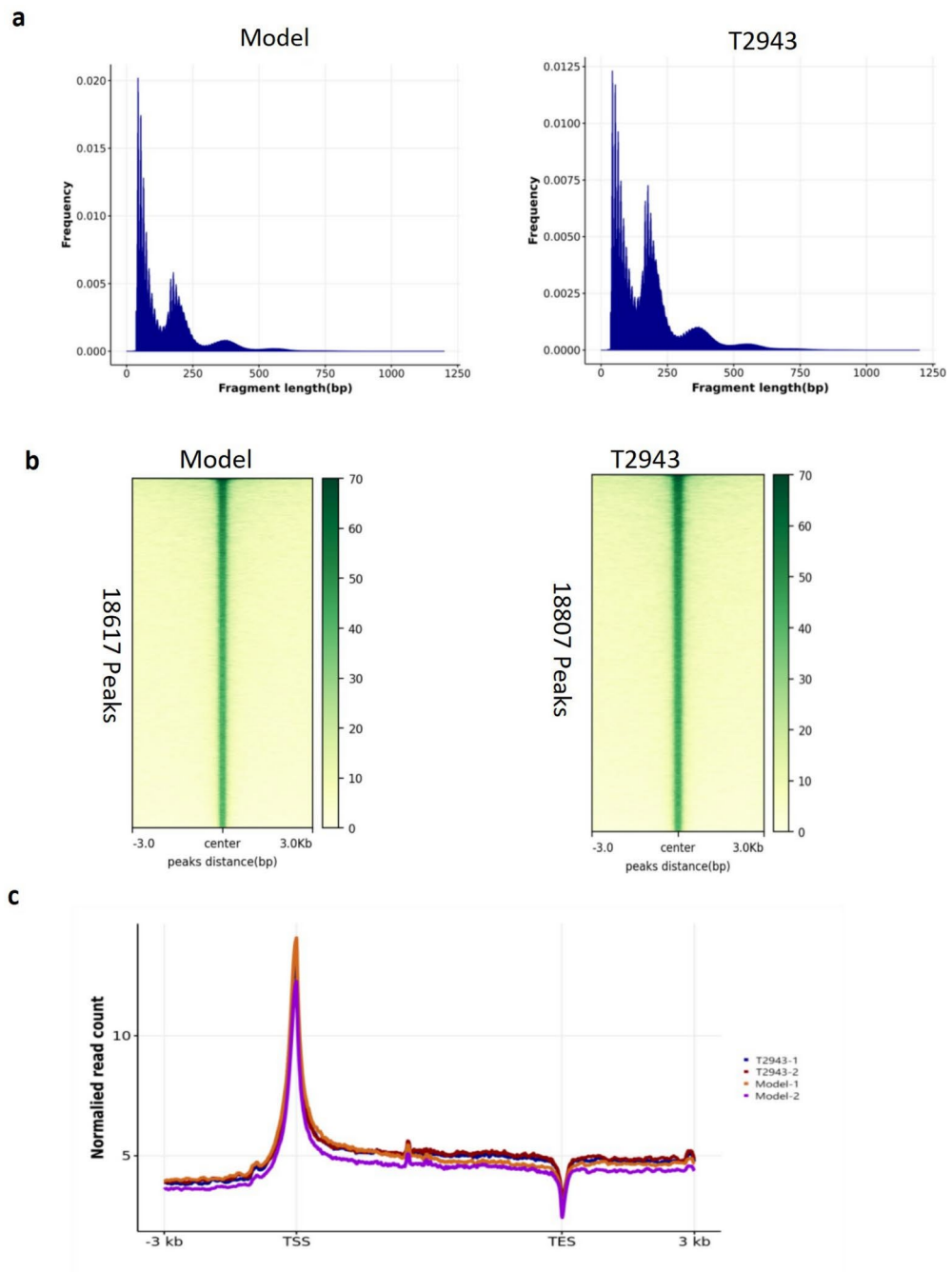


Fig. 1. CUT&Tag analysis of the hippocampi of the depression model and T2943 groups. **(a)** Fragment lengths in each group. **(b)** Heatmap showing the binding sites of H3K14ac. **(c)** Read showing the signal distribution.

compared with the model group, the genes promoting the upregulation of expression in the T2943 group were mainly involved in signaling regulation.

Pathway enrichment analysis showed that, compared with the model group, the upregulated target genes in the T2943 group were mainly enriched in neuroactive ligand-receptor interaction and axon guidance (Fig. 3). This suggests that the compound T2943 is involved in the activation of neuroligand-receptor interactions and the function of axon growth orientation.

Gene set enrichment analysis of gene fragments regulated by T2943 in the promoter region

To identify the differential target genes enriched in the promoter region with the most significant expression enhancement in the T2943 group, we performed GSEA to compare and screen the target genes concentrated among the neural function regulatory pathway genes related to depression. The results of the GSEA plot (Fig. 4a) indicated that the genes upregulated in the T2943 group were associated with the long-term synaptic regulatory

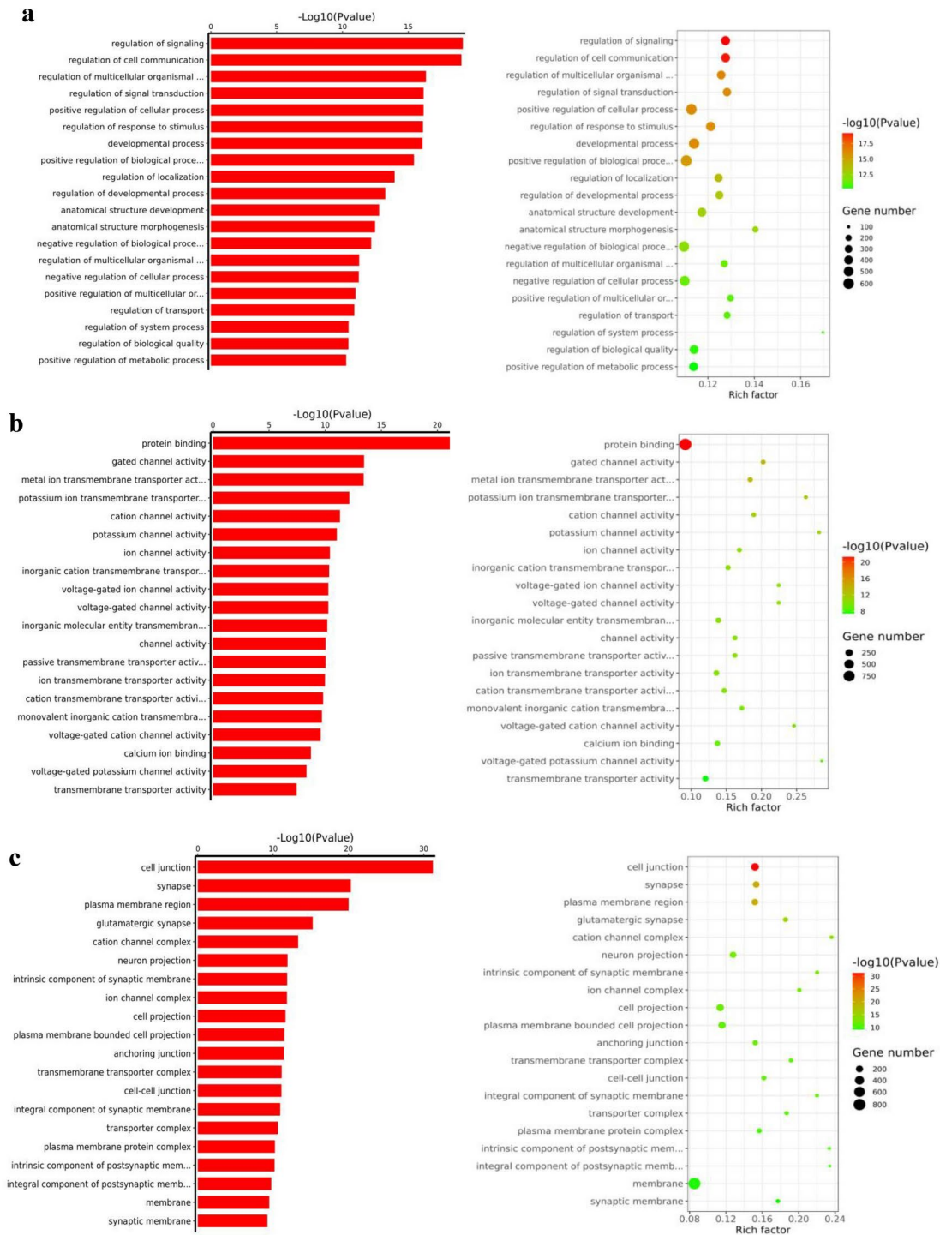


Fig. 2. GO analysis of enriched upregulated genes. The size of the dots represents the number of adjacent peak genes enriched in this GO entry, indicating that the signaling regulation in this GO entry involves a larger number of enriched genes. (a) Molecular function analysis. (b) Biological process analysis. (c) Cellular component analysis.

pathway of depression. As shown in the line plot of ESs (Fig. 4a), the concentrated genes were distributed at the top of the predefined gene set with a high ES. This suggested that the concentrated genes were closely associated with the gene-phenotype, while those immediately before the maximum ES were the core genes in the group.

Finally, each gene in the gene set was sequenced and counted according to fold change, and *Grid2* was identified as the core gene (Fig. 4b).

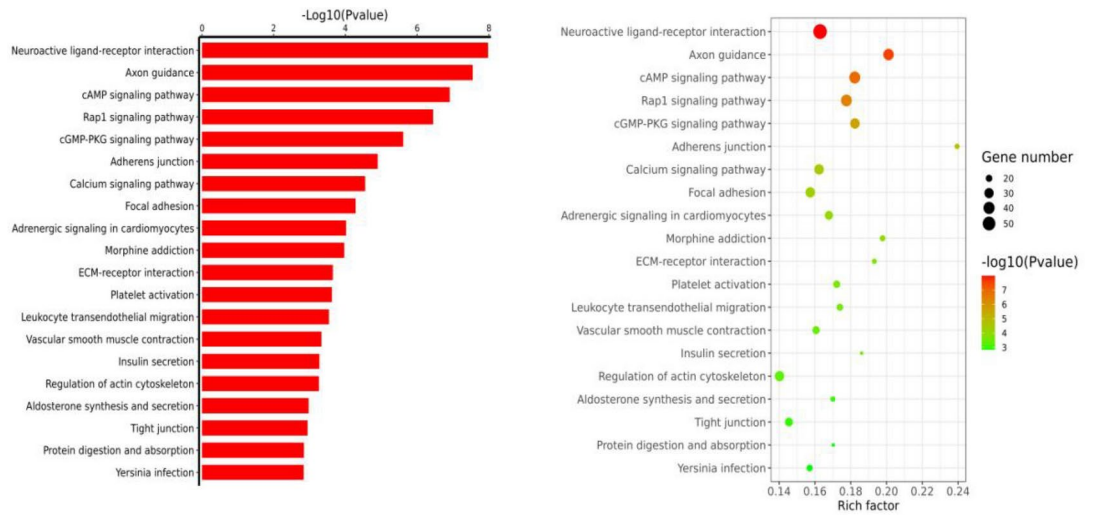
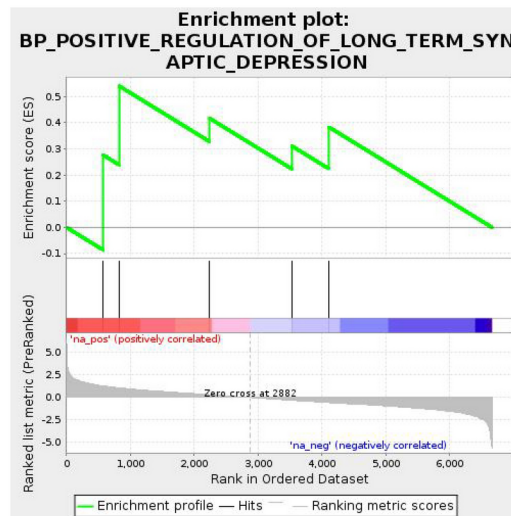


Fig. 3. Pathway analysis of enriched upregulated genes.

a



b

RANK	PROBE	RANK METRIC SCORE	RUNNING ES	CORE ENRICHMENT
1	GRID2	1.301902294	0.27709773	Yes
2	KCNB1	1.08278501	0.54092693	Yes
3	PPP1R9A	0.319824219	0.41707358	No
4	STAU2	-0.314047873	0.3112814	No
5	APP	-0.572566807	0.38378385	No

Fig. 4. GSEA results. (a) Profile of enrichment scores. (b) Prediction of core genes regulated by T2943.

Effects of T2943 on Grid2 and Grid1 transcription and expression

The core gene *Grid2* was predicted by CUT&Tag analysis, and GSEA was confirmed using qPCR. In the qPCR experiments, there were no significant differences between *Grid2* transcription and expression in the hippocampi of the control, model, or T2943 groups (Fig. 5a). Considering that genes with homologous sequences and high similarity may have caused certain deviations in the CUT&Tag and GSEA results, we searched genes homologous to *Grid2* on the NCBI website and found that *Grid1* and *Grid2* shared high similarity, with sequence homology reaching 99.31%. Therefore, we speculated that the core gene was likely *Grid1* rather than *Grid2*. We conducted qPCR experiments on *GRID1* and found that T2943 upregulated its expression (Fig. 5a); the same results were obtained with western blotting (Fig. 5b). Finally, immunofluorescence experiments in mouse hippocampi showed that T2943 promoted *Grid1* expression in granule cells in the DG region in all groups (Fig. 5c). These results confirmed that *Grid1*, rather than *Grid2*, is the core gene upregulated by T2943.

Knockdown of Grid1 expression abolishes or occludes the antidepressant-like effect of T2943

To confirm that T2943 exerts its antidepressant effect by increasing GRID1 expression, we tested whether *Grid1* knockdown influences antidepressant behavioral responses to T2943. We infused adeno-associated virus decreasing GRID1 expression (AAV-shGRID1) into granule cells of the DG. Compared with its effects in the control AAV-Vector mice, T2943 treatment did not affect the behavior of AAV-shGRID1 mice, as immobility duration in the TST, the distance in the central zone in the OFT, and the amount of sucrose consumed in the SPT were not altered in this group (Fig. 6a–c).

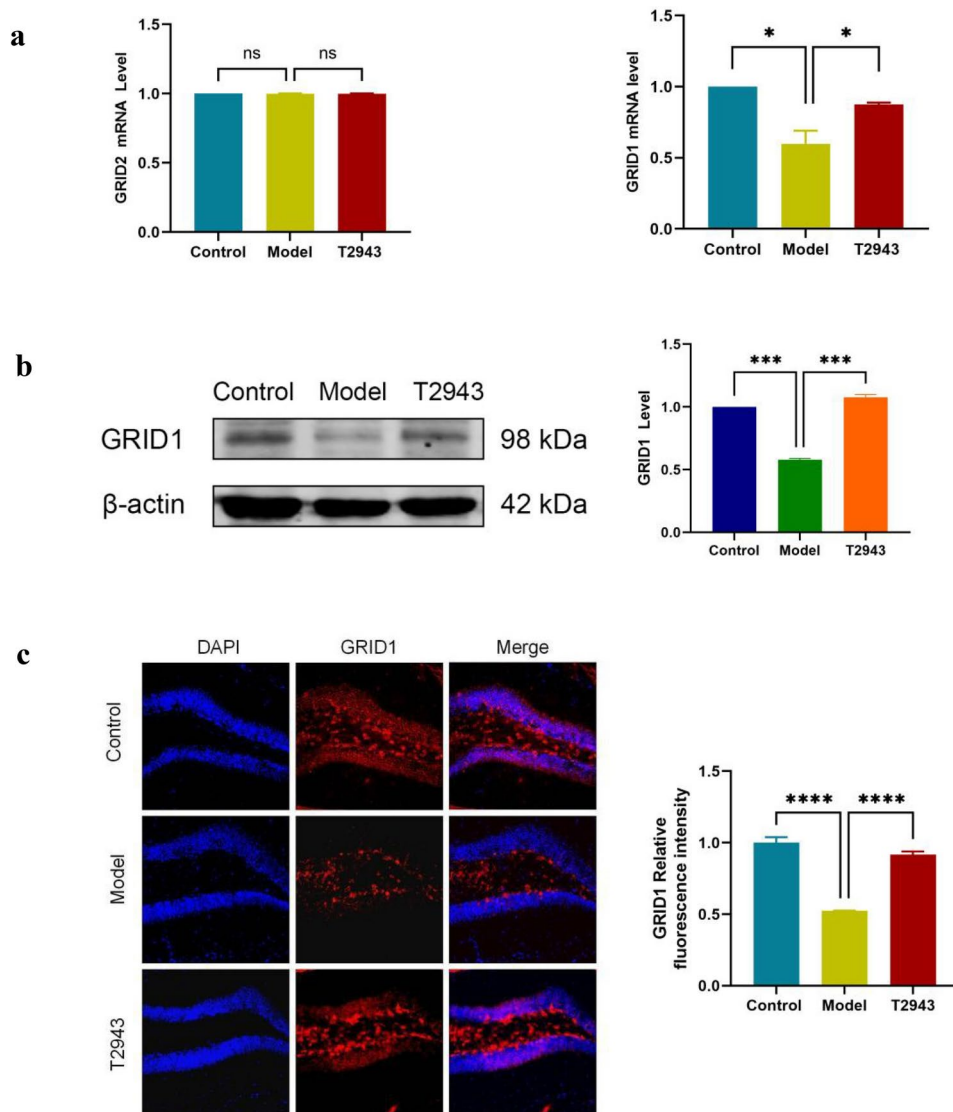


Fig. 5. GRID1 and GRID2 expression. (a) *Grid1* and *Grid2* mRNA expression using qPCR (n = 3). (b) GRID1 expression evaluation using western blot (n = 3)(original gels are presented in Supplementary Fig. 1). (c) GRID1 expression using immunofluorescence (n = 3).

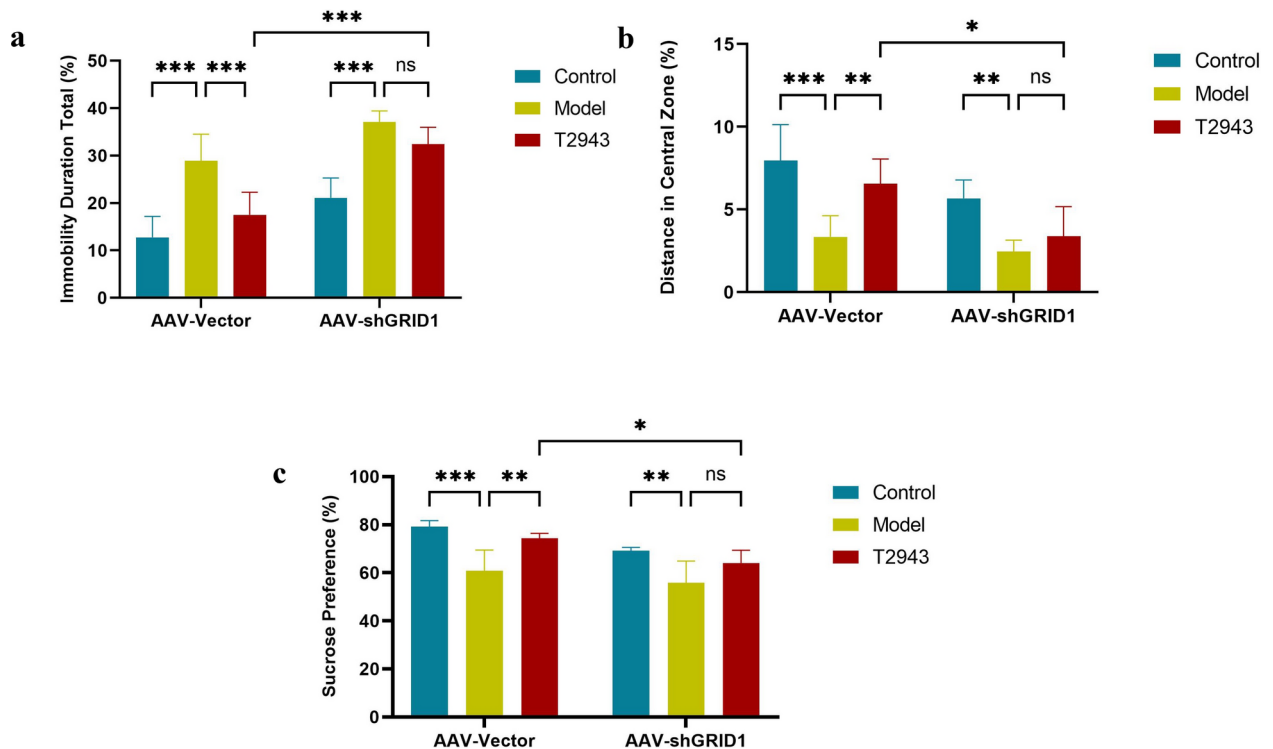


Fig. 6. T2943 treatment had no antidepressant effect in mice lacking *Grid1* expression in the hippocampus. (a) Immobility duration in the TST. (b) Distance in the central zone in the OFT. (c) Amount of sucrose consumed in the SPT. * $P < 0.05$, ** $P < 0.01$, *** $P < 0.001$.

These findings indicate that the antidepressant effects of T2943 are blocked by AAV-shGRID1 infusion, and therefore, T2943 exerts antidepressant effects by increasing GRID1 expression in vivo.

Discussion

The pathogenesis of depression is not fully understood. Previous studies have reported a link between depression and HDAC5, which is associated with chromatin deacetylation and regulates gene expression²⁷. HDAC5 plays an important role in various physiological and pathological processes²³. Environmental factors may affect HDAC5 expression. For example, adverse environmental conditions such as chronic stress and social isolation are believed to be important factors contributing to depression²⁸, and these adverse factors may affect the pathogenesis of depression by increasing HDAC5 levels^{21,22}.

HDAC5 inhibitors can be used for treating depression. Indeed, previous studies have confirmed the therapeutic potential of HDAC5 inhibitors in depression using animal models and clinical trials. HDAC5 inhibitors significantly improve behavioral performance in mice and alleviate depressive symptoms^{15,29}. In human clinical trials, HDAC5 inhibitors have shown effective antidepressant efficacy, with positive impacts on the emotional and psychological states of patients^{14,30}.

HDAC5 inhibitors exhibit therapeutic effects by increasing the expression of neurotrophic factors in neurons, which helps to protect neurons from damage and stimulate neuronal growth^{31,32}. In addition, HDAC5 inhibitors can regulate neurotransmitter levels in the brain, such as serotonin and dopamine³³, which are important for maintaining emotional balance.

Earlier, we discovered a novel HDAC5 inhibitor, T2943, and confirmed its anti-depressive effects in animal experiments. Using histone acetylation proteomic analysis, we found that T2943 promoted histone H3K14 acetylation by inhibiting HDAC5, thereby upregulating the H3K14ac level. In the present study, we investigated the core gene ultimately responsible for the anti-depressive effect of T2943 mediated via modulating H3K14ac expression. When H3K14 undergoes acetylation, its nucleosomal chromatin structure becomes relatively loose, which facilitates the recruitment of transcription factors to the promoter region of the target genes, promoting their transcription and expression. Comprehensive analysis using techniques such as CUT&Tag, GSEA, and behavioral tests after *Grid1* knockdown confirmed *Grid1* as the core gene associated with the anti-depressive effect of T2943. Based on our results, we propose that T2943 exerts antidepressant effects by regulating neural signaling pathways, promoting synaptic growth, or activating ligand-receptor interactions.

GRID1, also known as GluD1, belongs to one of the four major families of glutamate ion receptors, namely N-methyl-D-aspartate receptors (NMDAR), α -amino-3-hydroxy-5-methyl-4-isoxazole receptors (AMPA), kainic acid receptors, and ionic glutamate GluD receptors. Typically, these glutamate receptors are coupled to an ion channel, forming a receptor-channel complex that mediates rapid information transmission in the neuronal network. In rodents, GluD1 is expressed in multiple brain regions, including the cortex, hippocampus,

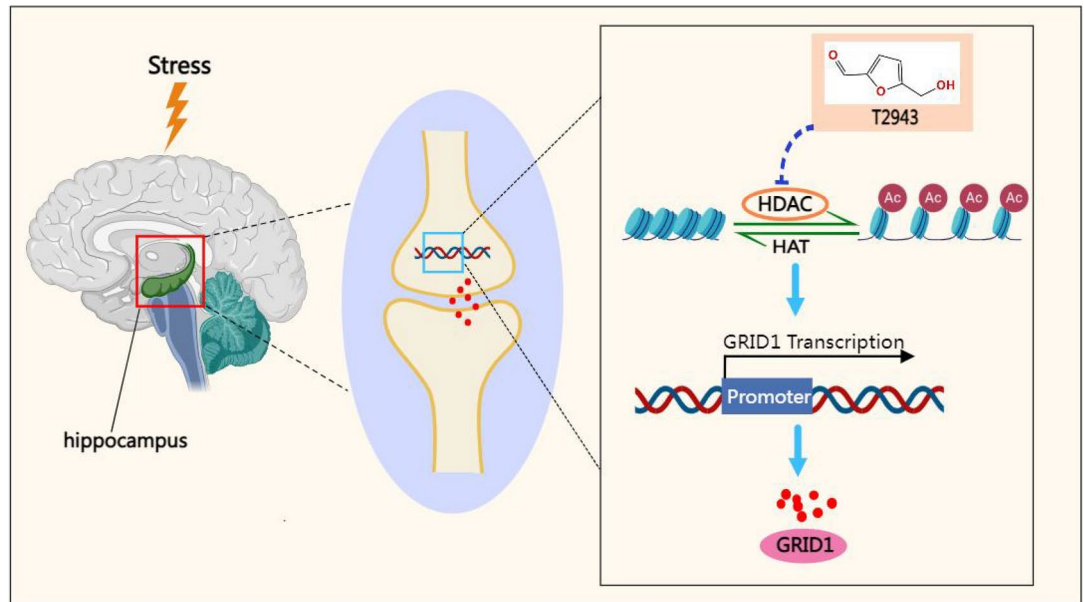


Fig. 7. Proposed mechanism underlying the anti-depressive effects of T2943.

amygdala, striatum, thalamus, nucleus accumbens, lateral hooked nucleus, and dorsal raphe nucleus^{34,35}. It is primarily expressed in the granule cells of the DG of the hippocampus^{34–37}.

Hippocampal DG granule cells are among the main sites of new neurons in the adult brain³⁸. The newly formed neurons in the hippocampus are mainly integrated into the granule cell layer and participate in learning, memory, and emotion regulation^{36,37}, including relieving stress and participating in the process of neuropsychiatric drug action³⁹. Hippocampal neurons have been linked to mental disorders⁴⁰. Moreover, compared with healthy individuals, patients with severe depression have fewer new neurons and a decrease in neurogenic niche vascularization. Adult nerve regeneration is influenced by various internal and external factors, such as behavior, emotion, age, and pathophysiological state, as well as external factors, such as the growth microenvironment of neural stem cells, drugs, and the environment.

Antidepressants enhance the ability of hippocampal DG neurons to regenerate; in a mouse model of depression, radiation damage experiments on the DG neurons showed that antidepressants did not reverse depressive symptoms in stem cell-deficient mice⁴¹. This finding suggests that antidepressants function via activating neural cell regeneration in the hippocampus. The GluD receptor family members expressed on hippocampal granule cells are crucial for the formation, maturation, and maintenance of synapses in the central nervous system and are associated with the occurrence and development of neurological diseases, including schizophrenia, depression, cognitive impairment, autism, and neurodevelopment^{42,43}. In human genome-wide association studies, low GluD1 expression has been linked to severe depression^{44,45}. GluD1-knockout mice exhibited depression, pleasure deficiency, hyperactivity disorder, reduced anxiety-like behavior, increased aggressive behavior, and social interaction deficits⁴⁶. When GluD1 deficiency results in impaired dendritic spine pruning, GluN2A is converted to the GluN2B subunit in the prefrontal cortex⁴⁷ and LIMK1 cofilin signaling changes in the hippocampus⁴⁸. In addition, blocking the mGluR5 signaling pathway in GluD1-knockout mice and inhibiting the Homer mGluR5 interaction inhibits the mGluR5-mediated Akt/mTOR signaling pathway related to depression⁴⁹. These results indicate that the downregulation of GluD1 expression *in vivo* is related to depression onset.

In terms of synaptic plasticity, current research has elucidated a relationship between the downregulation of GluD1 gene expression and the occurrence of depression. The amino terminal region of the GluD1 receptor binds to the cerebellin (Cbln) protein, which binds to the presynaptic neurexin (Nrxn) family, forming a complex of three binding molecules that exist in the synaptic gap and connect the presynaptic and postsynaptic regions⁵⁰. GRID1 and Cblns play significant synaptic roles in the hippocampus; GluD receptors in this region may specify synaptic targets for Cbln-expressing neurons or mediate connections between pyramidal cells in the hippocampus to regulate excitatory transmission. Moreover, they enhance excitatory synaptic transmission in the hippocampus by increasing the number of functional synapses to increase N-methyl-D-aspartate (NMDA) excitatory postsynaptic currents⁵¹. GRID1 overexpression can also increase inhibitory postsynaptic currents, indicating that GluD1 is necessary for normal synaptic function⁵². However, the effect of T2943 on synaptic plasticity, and its mechanisms, require further exploration and study.

Conclusion

Our study identifies a novel antidepressant compound, T2943, and elucidates the epigenetic mechanism by which it promotes the expression of Grid1. We propose that upregulated GRID1 mediates the transmission of synaptic signals in the neural pathway, restores the regenerative ability of hippocampal neurons, promotes nerve

growth and synaptic formation, increases the number of synapses, and enhances synaptic function to produce anti-depressive effects (Fig. 7).

We believe that our findings have important implications for the development of novel antidepressant therapies and contribute to a deeper understanding of the molecular pathways involved in depression. However, the treatment of depression using HDAC5 inhibitors remains in the early stages; therefore, more experimental and clinical data are needed to verify the safety and effectiveness of these compounds. Although some challenges remain in the treatment of depression with HDAC5 inhibitors, they are a potentially effective strategy for future application in clinical settings.

Data availability

The data that support the findings of this study are available from the corresponding author upon reasonable request.

Received: 11 August 2024; Accepted: 29 January 2025

Published online: 06 February 2025

References

- Smith, K. Mental health: A world of depression. *Nature* **515**, 181 (2014).
- Marwaha, S. et al. Novel and emerging treatments for major depression. *Lancet* **401**, 141–153 (2023).
- Burcusa, S. L. & Iacono, W. G. Risk for recurrence in depression. *Clin. Psychol. Rev.* **27**, 959–985 (2007).
- Saveanu, R. V. & Nemeroff, C. B. Etiology of depression: Genetic and environmental factors. *Psychiatr. Clin. North Am.* **35**, 51–71 (2012).
- Bruce, M. L. Psychosocial risk factors for depressive disorders in late life. *Biol. Psychiatry* **52**, 175–184 (2002).
- Cheptou, P. O. & Donohue, K. Epigenetics as a new avenue for the role of inbreeding depression in evolutionary ecology. *Heredity (Edinb)* **110**, 205–206 (2013).
- Shapero, B. G. et al. Stressful life events and depression symptoms: The effect of childhood emotional abuse on stress reactivity. *J. Clin. Psychol.* **70**, 209–223 (2014).
- Sun, H., Kennedy, P. J. & Nestler, E. J. Epigenetics of the depressed brain: Role of histone acetylation and methylation. *Neuropsychopharmacology* **38**, 124–137 (2013).
- Lin, E. & Tsai, S. J. Epigenetics and depression: An update. *Psychiatry Investig.* **16**, 654–661 (2019).
- Mill, J. & Petronis, A. Molecular studies of major depressive disorder: The epigenetic perspective. *Mol. Psychiatry* **12**, 799–814 (2007).
- Januar, V., Saffery, R. & Ryan, J. Epigenetics and depressive disorders: A review of current progress and future directions. *Int. J. Epidemiol.* **44**, 1364–1387 (2015).
- Narita, T., Weinert, B. T. & Choudhary, C. Functions and mechanisms of non-histone protein acetylation. *Nat. Rev. Mol. Cell Biol.* **20**, 156–174 (2019).
- Ropero, S. & Esteller, M. The role of histone deacetylases (HDACs) in human cancer. *Mol. Oncol.* **1**, 19–25 (2007).
- Park, H. S., Kim, J., Ahn, S. H. & Ryu, H. Y. Epigenetic targeting of histone deacetylases in diagnostics and treatment of depression. *Int. J. Mol. Sci.* **22**, 5398 (2021).
- Baek, S. Y. et al. Development of a novel histone deacetylase inhibitor unveils the role of HDAC11 in alleviating depression by inhibition of microglial activation. *Biomed. Pharmacother.* **166**, 115312 (2023).
- Guan, J. S. et al. HDAC2 negatively regulates memory formation and synaptic plasticity. *Nature* **459**(7243), 55–60 (2009).
- Lenoir, O. et al. Specific control of pancreatic endocrine β - and δ -cell mass by class IIa histone deacetylases HDAC4, HDAC5, and HDAC9. *Diabetes* **60**(11), 2861–2871 (2011).
- Daneshpajooh, M. et al. HDAC7 is overexpressed in human diabetic islets and impairs insulin secretion in rat islets and clonal beta cells. *Diabetologia* **60**(1), 116–125. <https://doi.org/10.1007/s00125-016-4113-2> (2017).
- Ito, K. et al. Decreased histone deacetylase activity in chronic obstructive pulmonary disease. *N. Engl. J. Med.* **352**(19), 1967–1976 (2005).
- Haberland, M., Montgomery, R. L. & Olson, E. N. The many roles of histone deacetylases in development and physiology: Implications for disease and therapy. *Nat. Rev. Genet.* **10**, 32–42 (2009).
- Iga, J. I. et al. Altered HDAC5 and CREB mRNA expressions in the peripheral leukocytes of major depression. *Prog. Neuropsychopharmacol. Biol. Psychiatry* **31**, 628–632 (2007).
- Hobara, T. et al. Altered gene expression of histone deacetylases in mood disorder patients. *J. Psychiatr. Res.* **44**, 263–270 (2010).
- Tsankova, N. M. et al. Sustained hippocampal chromatin regulation in a mouse model of depression and antidepressant action. *Nat. Neurosci.* **9**, 519–525 (2006).
- Covington, H. E. et al. Antidepressant actions of histone deacetylase inhibitors. *J. Neurosci.* **29**, 11451–11460 (2009).
- Du, J. et al. Antidepressant effect of the novel histone deacetylase-5 inhibitor T2943 in a chronic restraint stress mouse model. *Biomed. Pharmacother.* **171**, 116176 (2024).
- McLean, C. Y. et al. Great improves functional interpretation of cis-regulatory regions. *Nat. Biotechnol.* **28**, 495–501 (2010).
- Huang, W. et al. Acetate supplementation produces antidepressant-like effect via enhanced histone acetylation. *J. Affect. Disord.* **281**, 51–60 (2021).
- Erburu, M. et al. Chronic mild stress and imipramine treatment elicit opposite changes in behavior and in gene expression in the mouse prefrontal cortex. *Pharmacol. Biochem. Behav.* **135**, 227–236 (2015).
- Suo, H. et al. NRSF is an essential mediator for the neuroprotection of trichostatin A in the MPTP mouse model of Parkinson's disease. *Neuropharmacology* **99**, 67–78 (2015).
- McIntyre, R. S. et al. Bipolar disorders. *Lancet* **396**, 1841–1856 (2020).
- Watanabe, S. Y. et al. Gene expression-based biological test for major depressive disorder: an advanced study. *Neuropsychiatr. Dis. Treat.* **13**, 535–541 (2017).
- Ribeiro, A. C. R. et al. Epigenetic histone acetylation and Bdnf dysregulation in the hippocampus of rats exposed to repeated, low-dose diisopropylfluorophosphate. *Life Sci.* **281**, 119765 (2021).
- Holloway, T. & González-Maeso, J. Epigenetic mechanisms of serotonin signaling. *ACS Chem. Neurosci.* **6**, 1099–1109 (2015).
- Konno, K. et al. Enriched expression of GluD1 in higher brain regions and its involvement in parallel fiber-interneuron synapse formation in the cerebellum. *J. Neurosci.* **34**, 7412–7424 (2014).
- Hepp, R. et al. Glutamate receptors of the delta family are widely expressed in the adult brain. *Brain Struct. Funct.* **220**, 2797–2815 (2015).
- Balu, D. T. & Lucki, I. Adult hippocampal neurogenesis: Regulation, functional implications, and contribution to disease pathology. *Neurosci. Biobehav. Rev.* **33**, 232–252 (2009).

37. Pathania, M., Yan, L. D. & Bordey, A. A symphony of signals conducts early and late stages of adult neurogenesis. *Neuropharmacology* **58**, 865–876 (2010).
38. Abrous, D. N., Koehl, M. & Le Moal, M. Adult neurogenesis: From precursors to network and physiology. *Physiol. Rev.* **85**, 523–569 (2005).
39. Duan, X. et al. Disrupted-in-schizophrenia 1 regulates integration of newly generated neurons in the adult brain. *Cell* **130**, 1146–1158 (2007).
40. Kempermann, G., Krebs, J. & Fabel, K. The contribution of failing adult hippocampal neurogenesis to psychiatric disorders. *Curr. Opin. Psychiatry* **21**, 290–295 (2008).
41. Anacker, C. et al. Hippocampal neurogenesis confers stress resilience by inhibiting the ventral dentate gyrus. *Nature* **559**, 98–102 (2018).
42. Elegheert, J. et al. Structural basis for integration of GluD receptors within synaptic organizer complexes. *Science* **353**, 295–299 (2016).
43. Yuzaki, M. & Aricescu, A. R. A GluD coming-of-age story. *Trends Neurosci.* **40**, 138–150 (2017).
44. Muglia, P. et al. Genome-wide association study of recurrent major depressive disorder in two European case-control cohorts. *Mol. Psychiatry* **15**, 589–601 (2010).
45. Edwards, A. C. et al. Genome-wide association study of comorbid depressive syndrome and alcohol dependence. *Psychiatr. Genet.* **22**, 31–41 (2012).
46. Yadav, R. et al. Deletion of glutamate delta-1 receptor in mouse leads to aberrant emotional and social behaviors. *PLOS ONE* **7**, e32969 (2012).
47. Gupta, S. C. et al. Essential role of GluD1 in dendritic spine development and GluN2B to GluN2a NMDAR subunit switch in the cortex and hippocampus reveals ability of GluN2B inhibition in correcting hyperconnectivity. *Neuropharmacology* **93**, 274–284 (2015).
48. Yadav, R. et al. Deletion of glutamate delta-1 receptor in mouse leads to enhanced working memory and deficit in fear conditioning. *PLOS ONE* **8**, e60785 (2013).
49. Suryavanshi, P. S. et al. Glutamate delta-1 receptor regulates metabotropic glutamate receptor 5 signaling in the hippocampus. *Mol. Pharmacol.* **90**, 96–105 (2016).
50. Nakamoto, C. et al. GluD1 knockout mice with a pure C57BL/6N background show impaired fear memory, social interaction, and enhanced depressive-like behavior. *PLOS ONE* **15**, e0229288 (2020).
51. Tao, W., Díaz-Alonso, J., Sheng, N. & Nicoll, R. A. Postsynaptic $\delta 1$ glutamate receptor assembles and maintains hippocampal synapses via Cbln2 and neuroligin. *Proc. Natl Acad. Sci. U. S. A.* **115**, E5373–E5381 (2018).
52. Fossati, M. et al. Trans-synaptic signaling through the glutamate receptor delta-1 mediates inhibitory synapse formation in cortical pyramidal neurons. *Neuron* **104**, 1081–1094 (2019).

Acknowledgements

This work was supported by the Major Research Development Program of Ningxia Hui Autonomous Region (Grant number: 2022BEG02043), the Major Research Development Program of Ningxia Hui Autonomous Region (Grant number: 2022BEG02042), the Research Project of the Key Laboratory of Protection, Development, and Utilization of Medicinal Resources in the Liupanshan Area, Ministry of Education (Grant number: KFKT202312), Natural Science Foundation of Ningxia Hui Autonomous Region (Grant number: 2024AAC03237), and the National Natural Science Foundation of China (Grant number: 82260232).

Author contributions

Study conception and design: Jianqiang Yu, Qiuhua Cao, Ning Liu. Methodology: Juan Du. Validation: Ruyun Liu, Lin Ma. Resources: Juan Du, Ning Liu, Lin Ma. Investigation: Juan Du, Yue Liu, Wei Wei. Project administration: Juan Du. Data Curation: Yue Liu, Wei Wei. Writing – Original Draft: Juan Du. Writing – Review & Editing: Ruyun Liu, Lin Ma, Yue Liu, Wei Wei, Jianqiang Yu, Qiuhua Cao, Ning Liu. Supervision: Jianqiang Yu, Qiuhua Cao, Ning Liu.

Declarations

Competing interests

The authors declare no competing interests.

Additional information

Supplementary Information The online version contains supplementary material available at <https://doi.org/10.1038/s41598-025-88670-5>.

Correspondence and requests for materials should be addressed to N.L., Q.C. or J.Y.

Reprints and permissions information is available at www.nature.com/reprints.

Publisher's note Springer Nature remains neutral with regard to jurisdictional claims in published maps and institutional affiliations.

Open Access This article is licensed under a Creative Commons Attribution-NonCommercial-NoDerivatives 4.0 International License, which permits any non-commercial use, sharing, distribution and reproduction in any medium or format, as long as you give appropriate credit to the original author(s) and the source, provide a link to the Creative Commons licence, and indicate if you modified the licensed material. You do not have permission under this licence to share adapted material derived from this article or parts of it. The images or other third party material in this article are included in the article's Creative Commons licence, unless indicated otherwise in a credit line to the material. If material is not included in the article's Creative Commons licence and your intended use is not permitted by statutory regulation or exceeds the permitted use, you will need to obtain permission directly from the copyright holder. To view a copy of this licence, visit <http://creativecommons.org/licenses/by-nc-nd/4.0/>.

© The Author(s) 2025